

Epitaxial refractory-metal buffer layers with a chemical gradient for adjustable lattice parameter and controlled chemical interface

O. Fruchart, A. Rousseau, D. Schmaus, A. L'Hoir, R. Haettel, and L. Ortega

Citation: *Applied Physics Letters* **98**, 131906 (2011); doi: 10.1063/1.3567793

View online: <http://dx.doi.org/10.1063/1.3567793>

View Table of Contents: <http://scitation.aip.org/content/aip/journal/apl/98/13?ver=pdfcov>

Published by the *AIP Publishing*

Articles you may be interested in

Long wavelength emitting GaInN quantum wells on metamorphic GaInN buffer layers with enlarged in-plane lattice parameter

Appl. Phys. Lett. **105**, 111111 (2014); 10.1063/1.4895067

Control of epitaxial growth of Fe-based nanocrystals on Si substrates using well-controlled nanometer-sized interface

J. Appl. Phys. **115**, 044301 (2014); 10.1063/1.4862642

Effects of the TiO₂ buffer thickness on SrTiO₃ (111) epitaxial films grown on GaN (0002)

J. Appl. Phys. **113**, 154103 (2013); 10.1063/1.4801804

Structural and magnetic properties of La_{0.7}Sr_{0.3}MnO₃ thin films integrated onto Si(100) substrates with SrTiO₃ as buffer layer

J. Appl. Phys. **109**, 07C120 (2011); 10.1063/1.3565422

Metamorphic In As_yP_{1-y} (y = 0.30 – 0.75) and Al_δIn_{1-δ}As_yP_{1-y} buffer layers on InP substrates

Appl. Phys. Lett. **90**, 212113 (2007); 10.1063/1.2742649



NEW Special Topic Sections

NOW ONLINE
Lithium Niobate Properties and Applications:
Reviews of Emerging Trends

AIP | Applied Physics Reviews

Epitaxial refractory-metal buffer layers with a chemical gradient for adjustable lattice parameter and controlled chemical interface

O. Fruchart,^{1,a)} A. Rousseau,¹ D. Schmaus,² A. L'Hoir,² R. Haettel,¹ and L. Ortega¹

¹*Institut Néel, CNRS and Université Joseph Fourier, BP166, F-38042 Grenoble Cedex 9, France*

²*Institut des NanoSciences de Paris (INSP), CNRS UMR 7588, UPMC Université Paris 6, 4 place Jussieu, 75252 Paris Cedex 05, France and Université Paris Diderot-Paris 7, 75205 Paris Cedex 13, France*

(Received 23 January 2011; accepted 26 February 2011; published online 30 March 2011)

We have developed and characterized the structure and composition of nanometers-thick solid-solution epitaxial layers of (V,Nb) on sapphire (11 $\bar{2}$ 0), displaying a continuous lateral gradient of composition from one to another pure element. Further covered with an ultrathin pseudomorphic layer of W, these provide a template for the fast combinatorial investigation of growth or physical properties depending of strain. © 2011 American Institute of Physics. [doi:10.1063/1.3567793]

Thin films play a crucial role in integrated technology. While in a down-scaling approach one seeks to sustain the bulk properties, one may also endeavor to tailor properties that do not occur in the bulk, an approach being one basis for the development of nanosciences. A parameter often at play in the change in properties in thin films is strain,¹ influencing, e.g., mobility in semiconductors,² optical activity, electric polarization or magnetic moment,³ and anisotropy.⁴ The usual way to control strain in thin films is through their growth on substrates with a lattice parameter different from their own, inducing a so-called lattice misfit. Lattice misfit also influences growth modes (smooth or rough films, islands, etc.).^{5,6} This shows the need for its control.

Effects of lattice misfit are often investigated by growth on single crystals of various pure elements, each with a well-defined lattice parameter. Alloys and solid solutions (ss) are an appealing combinatorial alternative as they allow for the continuous control of lattice misfit, which is not possible for pure elements.⁷ Nevertheless, systematic studies with ss require several samples with different compositions, with issues of time, reproducibility and limited number of data points. To circumvent this Kennedy *et al.*⁸ have introduced compositional spreads, where the anisotropy of evaporation of two or more sources are used to create a slight gradient of composition across a sample. Later, alternated deposition of the materials along with moving masks were used to create intercalated wedges of two or three elements.^{9,10} This allows one to vary the composition linearly and potentially from 0% up to 100%. In these seminal uses of masks the alloy resulted from a postannealing, which is not suited for most epitaxial thin films. Only Zhong *et al.*¹¹ applied this technique to epitaxial materials (semiconductors), however restricted it to the case of weak doping.

We issued a preliminary report of chemical gradients with controlled chemical surface,¹² however, with a negligible variation in lattice parameter via mixing body-centered cubic (bcc) Mo (lattice parameter 3.157 Å) and W (3.165 Å), therefore with virtually no metallurgical issues and with restricted practical use. Here we report the fabrication, the structural, composition, and surface characterization of epitaxial chemical-gradient layers (CGLs) of bcc refractory metals, in the full range of composition to adjust the lattice

parameter over 10%. Further combined with an ultrathin pseudomorphic layer, these provide a versatile buffer-layer toolkit for the elucidation and use of the many phenomena depending on lattice misfit.

The samples were grown using pulsed-laser deposition in a set of ultrahigh vacuum chambers. The laser is a 10 Hz Nd-YAG with pulse length ≈ 10 ns and doubled frequency ($\lambda = 532$ nm). The deposition chamber is equipped with a computer-controlled mask moving in front of the sample, and 10 kV reflection high energy electron diffraction (RHEED).¹² Our CGLs are based on mixtures of two bcc elements (Mo, W, Nb, V), that all form ss one with another. Results are illustrated in this Letter with the case of (V,Nb). (11 $\bar{2}$ 0) sapphire wafers are used as a support, resulting in the (110) texture of the films.^{12,13} Searching for an optimized procedure, CGLs were grown directly on 0.7-nm-thick Mo-dusted sapphire wafer (Mo is inserted to avoid crystallographic variants¹²), or on an atomically-flat 10-nm-thick W(110) buffer layer itself above Mo-dusted sapphire. The wedges of the two elements are deposited sequentially, in an opposite fashion thanks to the azimuthal rotation of the sample of 180°. The length of the wedges is 5 mm [Fig. 1(a)]. Their typical thickness is 1 Å, which is less than one atomic layer, with a view to promote the mixture of both elements at the atomic level and avoid the formation of misfit dislocations that would occur for thick individual layers. Deposition is performed at moderate temperature (300 °C), followed by annealing for 30 min at 800 °C. The typical total thickness of these films is 10 nm.

Figure 1 shows RHEED patterns and scanning tunneling microscopy (STM) images of a (V,Nb)/Mo(0.7 nm) CGL directly grown on sapphire. The RHEED streak narrowness, large terrace size and absence of emerging screw dislocations, provide a picture of a high-quality crystal. No significant difference is found in RHEED and STM data as a function of the local composition, from pure V to pure Nb, with or without an underlying W buffer layer.

We developed a sample holder to perform x-ray diffraction over a small and precise location on the sample. It consists of a 1 mm wide window between two steel blades machined at an angle of 12° to let in and out x-rays down to grazing incidence. The blades are covered with a 10- μ m-thick layer of metallic glass (Zr_{52.5}Ti_{2.5}Cu₂₂Ni₁₃Al₁₀) to avoid diffraction from the mask. A manual sample trans-

^{a)}Electronic mail: olivier.fruchart@grenoble.cnrs.fr.

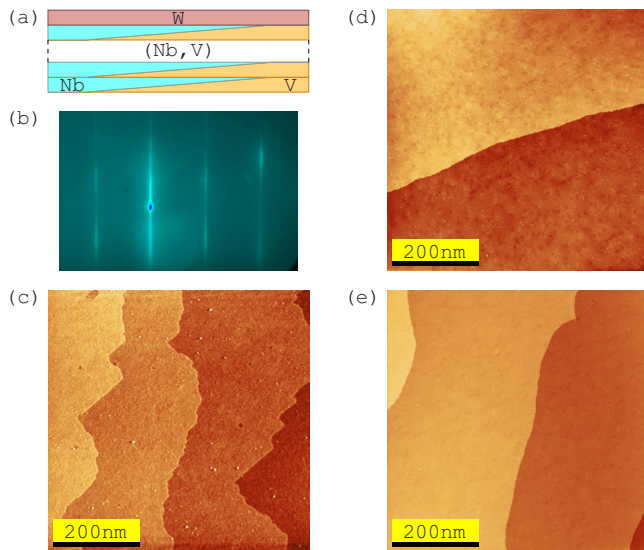


FIG. 1. (Color online) (a) Schematics of a CGL, further covered by an ultrathin W layer for the chemical control of the free surface. (b) typical RHEED pattern, for electron azimuth $[1\bar{1}0]$ (the bright spot is the reflected beam). STM images of (V,Nb)/Mo(0.7 nm)/Al₂O₃ CGLs (not covered with an ultrathin W layer) for (c) V, (d) V₅₀Nb₅₀ and (e) Nb.

lator allows one to select the area of investigation [inset of Fig. 2(a)]. Figure 2(a) shows $\theta-2\theta$ spectra as a function of location on the sample, translated into the expected composition. The occurrence of Kiessig fringes arises from the finite thickness of the films and the absence of roughness. Their width is composition-independent and consistent with

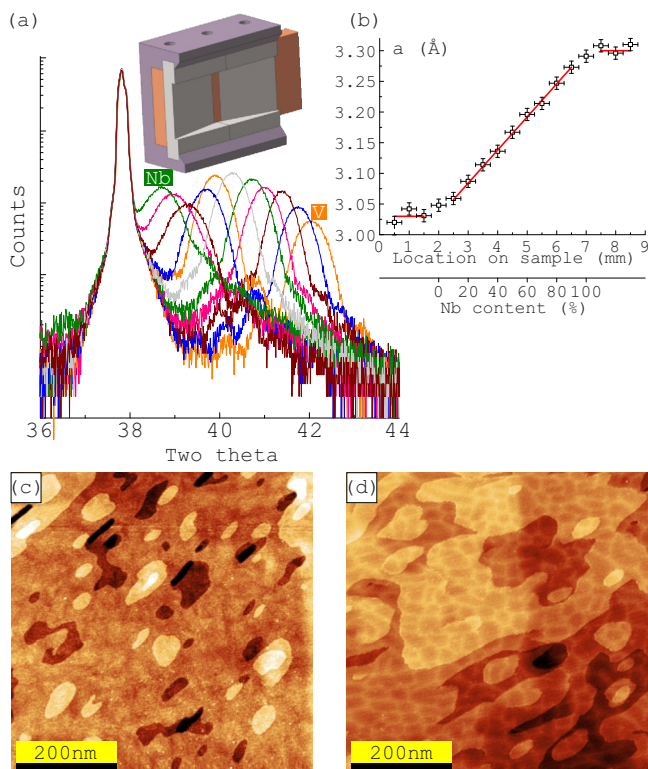


FIG. 2. (Color online) (a) $\theta-2\theta$ diffraction spectra of (V,Nb)/Mo(0.7 nm)/Al₂O₃ CGLs. At 37.85° is a sapphire peak. Inset: mask used to select the area of interest for diffraction (b) Extracted from (a), out-of-plane lattice parameter as a function of composition along the CGL. Lines are the expectation of Vegard's law. STM images of ultrathin layers of W of thickness (c) 0.6 nm and (d) 2 nm on a (V,Nb) CGL, both close to pure Nb.

the film thickness. The films are thus coherent across their entire thickness, showing their good layered structure, consistent with STM data [Figs. 1(c)–1(e)]. The out-of-plane lattice parameters extracted from these curves are shown in Fig. 2(b). The error bars result from the precision of the lateral position of the sample, and from the combined fitting of peaks and calibration of the diffractometer against the first and second order peaks of sapphire. Within the error bar the lattice parameter varies linearly with composition and ranges from the bulk lattice parameter of V (3.02 Å) to that of Nb (3.30 Å), in agreement with Vegard's law and consistent with the step height found with STM. *In situ* RHEED yields the in-plane lattice parameter, albeit with larger error bars (not shown here). These also fit Vegard's law, demonstrating the good structural relaxation of the ss. Finally, the CGLs may be covered by an ultrathin W layer deposited at 250 °C and then annealed at 800 °C, a procedure known not to give rise to intermixing with the underlying film.¹² For all compositions STM shows that W remains pseudomorphic up to ≈ 1 nm [see Fig. 2(c) for the case of W/Nb], above which relaxation is revealed by an array of misfit dislocations [Fig. 2(d)].¹⁴ CGLs covered with this ultrathin pseudomorphic W layer provide a surface with a continuously-variable lattice parameter, however, with a uniform and a rather inert surface material.

In order to check locally both the composition of the ss, and their crystalline quality, the samples were also analyzed using Rutherford backscattering spectrometry (RBS) both in random and channeling geometries (for these analytical techniques, see Ref. 15). Whereas X-ray and electron diffraction probe long-range crystalline coherence and are mostly insensitive to local disorder, RBS in a channeling geometry is highly sensitive to such disorder and is thus very valuable to refine the close-to-perfect picture of CGLs given by Figs. 1 and 2. RBS was performed within the SAFIR facility of the INSP, using a 1.4 MeV ⁴He⁺ ion beam with a 0.5 mm diameter, produced by a 2.5 MV van de Graaff accelerator. The ions scattered elastically at large angle (here $\approx 150^\circ$) on the sample nuclei (rare scattering events) were energy-analyzed using a silicon detector.

Conversely, the most probable scattering events result in small-angle repulsive deflections. When the incident beam is aligned with a major crystallographic axis of a crystal (channeling geometry, here performed along $[110]$), these deflections are correlated and the particle flux close to the rows is strongly reduced, leading to a similar reduction in the RBS yield Y with respect to the yield R using a random orientation of the beam. For convenience, in the following Y values are normalized to the corresponding RBS random yield. Whereas R_i values for element i are proportional to the absolute amount of i atoms in the layer, Y_i values are mostly sensitive to atomic displacements in the plane perpendicular to the channeling axis.¹⁶

Various samples were analyzed, but we only present here the case of (V,Nb) deposited on a 10 nm-thick W(110) buffer layer (Fig. 3). Both $R_V(x)$ and $R_{Nb}(x)$ exhibit a linear variation across the sample, their sum keeping a nearly constant value corresponding to a thickness of about 10 nm of the (Nb,V) layer. This provides a direct quantitative confirmation of the linear variation in composition [e.g., $C_{Nb} = R_{Nb}/(R_{Nb} + R_V)$] with x , suggested indirectly previously through the agreement with Vegard's law (Fig. 2).

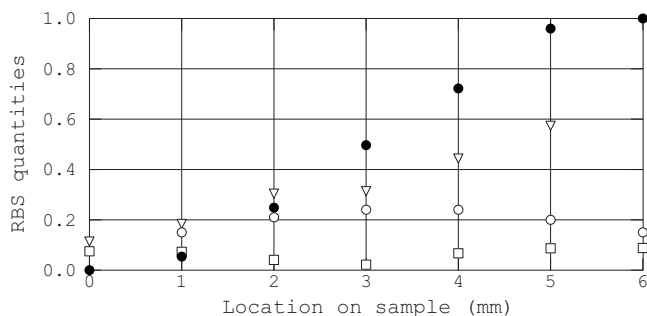


FIG. 3. Local quantities determined by RBS (random or channeling conditions), as a function of the location x across a (V,Nb)/W(10 nm)/Mo(0.7 nm)/Al₂O₃ CGL: Nb concentration (●), normalized channeling ([110] alignment) yields Y_{Nb} (○), Y_V (▽), and Y_W (□). The zero for the lateral scale is different from that of Fig. 2(b).

Concerning the crystalline quality of the ss, the relatively high channeling yields Y_{Nb} and Y_V observed on Fig. 3, with a marked dependence on C_{Nb} , may hint at atomic displacements in the ss, relatively far from the CGL-W interface (see below). Their precise identification needs further analysis. Despite this, paradoxically, the very low channeling yield Y_W in the range [0.02–0.05] is indicative of a very good epitaxy. The highest quality ($Y_W \approx 0.02$) is obtained for Nb_{0.5}V_{0.5}, for which there is no lattice misfit between the alloy and W, in agreement with Fig. 2(b).

To conclude, we developed high-quality epitaxial ss layers of refractory metals along the orientation (110), in the form of CGLs. These CGLs were then covered with a flat and ultrathin pseudomorphic layer of W(110). This combination provides a template with a lattice parameter varying laterally over 10% and with a controlled and rather inert W chemical interface, which may be used for the fast combinatorial investigation of any growth or physical phenomenon depending on strain. This may be performed with local probes such as electron, optical, or scanning-probe microscopies, or with many nowadays synchrotrons offering beams focused to 100 μ m or smaller. CGLs of metals should be feasible with other crystalline structures and/or orientation such as bcc(001).⁷ The best surface quality may

be expected for low interfacial interaction such as metal on oxide and for gliding plane parallel to the growth surface, so as to allow for the lattice relaxation through the introduction of interfacial dislocations, avoiding emerging screw dislocations. These conditions are fulfilled in the present case.

We acknowledge the help of J. L. Soubeyroux (CRETA, Grenoble) by providing bulk metallic glass for preliminary XRD slits, N. Dempsey (Institut Néel) for the deposition of thick films of metallic glass, V. Guisset and Ph. David for technical support with UHV, and E. Briand for efficient help in RBS experiments. This work received financial support from FP6 EU-NSF program (STRP 016447 MagDot) and French National Research Agency (Grant No. ANR-05-NANO-073 Vernanomag).

¹E. Newnham, *Properties of Materials: Anisotropy, Symmetry, Structure* (Oxford University Press, Oxford, 2005).

²M. V. Fischetti and S. E. Laux, *J. Appl. Phys.* **80**, 2234 (1996).

³V. L. Moruzzi, P. M. Marcus, and J. Kübler, *Phys. Rev. B* **39**, 6957 (1989).

⁴J. Buschbeck, I. Opahle, M. Richter, U. K. Röbber, P. Klaer, M. Kallmayer, H. J. Elmers, G. Jakob, L. Schultz, and S. Fähler, *Phys. Rev. Lett.* **103**, 216101 (2009).

⁵E. Bauer and J. H. Van der Merwe, *Phys. Rev. B* **33**, 3657 (1986).

⁶J. H. van der Merwe, *Philos. Mag. A* **45**, 159 (1982).

⁷P. Y. Friot, P. Turban, S. Andrieu, M. Piecuch, E. Snoeck, A. Traverse, E. Foy, and C. Theodorescu, *Eur. Phys. J. B* **15**, 41 (2000).

⁸K. Kennedy, T. Stefansky, G. Davy, C. F. Zackay, and E. R. Parker, *J. Appl. Phys.* **36**, 3808 (1965).

⁹F. Tsui and L. He, *Rev. Sci. Instrum.* **76**, 062206 (2005).

¹⁰V. Matias and B. J. Gibbons, *Rev. Sci. Instrum.* **78**, 072206 (2007).

¹¹Y. Zhong, Y. S. Chu, B. A. Collins, and F. Tsui, *Appl. Surf. Sci.* **254**, 714 (2007).

¹²O. Fruchart, P. O. Jubert, M. Eleoui, F. Cheynis, B. Borca, P. David, V. Santonacci, A. Liénard, M. Hasegawa, and C. Meyer, *J. Phys.: Condens. Matter* **19**, 053001 (2007).

¹³G. Oya, M. Koishi, and Y. Sawada, *J. Appl. Phys.* **60**, 1440 (1986).

¹⁴H. Bethge, D. Heuer, C. Jensen, K. Reshöft, and U. Köhler, *Surf. Sci.* **331–333**, 878 (1995).

¹⁵D. Schmaus and I. C. Vickridge, *Analytical Methods for Corrosion Science and Engineering*, (CRC/Taylor & Francis, Boca Raton, 2006), p. 103.

¹⁶A detailed discussion of RBS-channeling data will be addressed separately.